Passive Mixing in a Three-Dimensional Serpentine Microchannel

Robin H. Liu, Mark A. Stremler, Kendra V. Sharp, Michael G. Olsen, Juan G. Santiago, Ronald J. Adrian, Hassan Aref, and David J. Beebe, *Member, IEEE*

***Abstract*—A three-dimensional serpentine microchannel design with a "C-shaped" repeating unit is presented in this paper as a means of implementing chaotic advection to passively enhance fluid mixing. The device is fabricated in a silicon wafer using a double-sided KOH wet-etching technique to realize a three-dimensional channel geometry. Experiments using phenolphthalein and sodium hydroxide solutions demonstrate the ability of flow in this channel to mix faster and more uniformly than either pure molecular diffusion or flow in a "square-wave" channel for Reynolds numbers from 6 to 70. The mixing capability of the channel increases with increasing Reynolds number. At least 98% of the maximum intensity of reacted phenolphthalein is observed in the channel after five mixing segments for Reynolds numbers greater than 25. At a Reynolds number of 70, the serpentine channel produces 16 times more reacted phenolphthalein than a straight channel and 1.6 times more than the square-wave channel. Mixing rates in the serpentine channel at the higher Reynolds numbers are consistent with the occurrence of chaotic advection. Visualization of the interface formed in the channel between streams of water and ethyl alcohol indicates that the mixing is due to both diffusion and fluid stirring. [439]**

***Index Terms*—Chaotic advection, fluid mixing, microfuidics.**

I. Introduction

RAPID mixing is essential in many of the microfluidic systems targeted for use in biochemistry analysis, drug delivery, and sequencing or synthesis of nucleic acids, among others [1]–[3]. Biological processes such as cell activation, enzyme reactions, and protein folding often involve reactions that require mixing of reactants for initiation. Mixing is also necessary in many microfabricated chemical systems that carry out complex chemical synthesis [4], [5].

When the dimensions of a channel cross section are tens of micrometers, molecular diffusion can mix two fluid streams in just a few seconds. However, when the dimensions are several hundred micrometers, a molecular diffusion-based mixing process can take tens of seconds. Mixing is particularly inefficient in solutions containing macromolecules that have diffusion coefficients one or two orders of magnitude lower than that of most liquids [6]. Effective mixing at this scale requires that fluids be manipulated to increase the interfacial surface area between initially distinct fluid regions so that diffusion can complete the mixing process in a reasonable time. Unfortunately, the rapid mixing produced by turbulent flows is usually not available at the microscale because the Reynolds number (Re)[1] is typically below the critical value for transition to turbulence. Thus, some other mechanism must be used to enhance mixing.

The literature contains a number of devices designed to enhance mixing on the microscale. These devices fall into one of two categories: 1) active mixers [7]–[9] that exert some form of active control over the flow field through such means as moving parts or varying pressure gradients or 2) passive mixers [10]–[12] that utilize no energy input except the mechanism (pressure head or pump) used to drive the fluid flow at a constant rate. While active mixers can produce excellent mixing, they are often difficult to fabricate, operate, clean, and integrate into microfluidic systems. Thus, the focus here is on passive mixing because it is relatively simple to implement.

It has been shown that a "twisted pipe" has the potential to enhance mixing even at low Reynolds numbers [13]. This mixing enhancement is possible because of the phenomenon known as chaotic advection [14], [15], in which simple regular velocity fields produce chaotic particle trajectories. Dynamical systems theory shows that chaotic particle motion can occur when a velocity field is either two-dimensional and time-dependent or three-dimensional (with or without time dependence). The occurrence of chaotic advection typically indicates rapid distortion and elongation of material interfaces. This process significantly increases the area across which diffusion occurs, which leads to rapid mixing. On the macroscale, "twisted-pipe" configurations have proven to be very effective mixers for $\mathrm{Re} \geq 60$ [16]–[18]. Here we present a microchannel design based on the "twisted pipe" and document the mixing performance of the flow in this channel for Re from 6 to 70. A preliminary report on this work was presented at the International Transducers'99 Conference held in Sendai, Japan [19].

II. Design and Fabrication

In order to mix well at low Reynolds numbers, the geometry of a channel must be "complicated enough" that chaotic advec-

Manuscript received April 22, 1999; revised November 5, 1999. This work was supported by the Defense Advanced Research Projects Agency/Microsystems Technology Office μFlumes and Composite Computer-Aided-Design Programs. Subject Editor, D. J. Harrison.

R. H. Liu, M. A. Stremler, K. V. Sharp, M. G. Olsen, R. J. Adrian, and H. Aref are with the University of Illinois at Urbana-Champaign, Urbana, IL 61801 USA.

J. G. Santiago is with the Department of Mechanical Engineering, Stanford University, Palo Alto, CA 94305 USA.

D. J. Beebe was with the Department of Electrical and Computer Engineering, Beckman Institute for Advanced Science and Technology, University of Illinois at Urbana-Champaign, Urbana, IL 61801 USA. He is now with the Department of Biomedical Engineering, University of Wisconsin-Madison, Madison, WI 53706 USA.

Publisher Item Identifier S 1057-7157(00)04860-5.

[1]The Reynolds number gives the ratio between inertial forces and viscous forces in a flow. The definition used here is $\mathrm{Re} = (Q/A)D_h/\nu$, where Q is the volumetric flow rate through the channel, A is the cross-sectional area, and D_h is the hydraulic diameter of the channel ($4A$/wetted perimeter of the channel), and ν is the kinematic viscosity of the fluid.

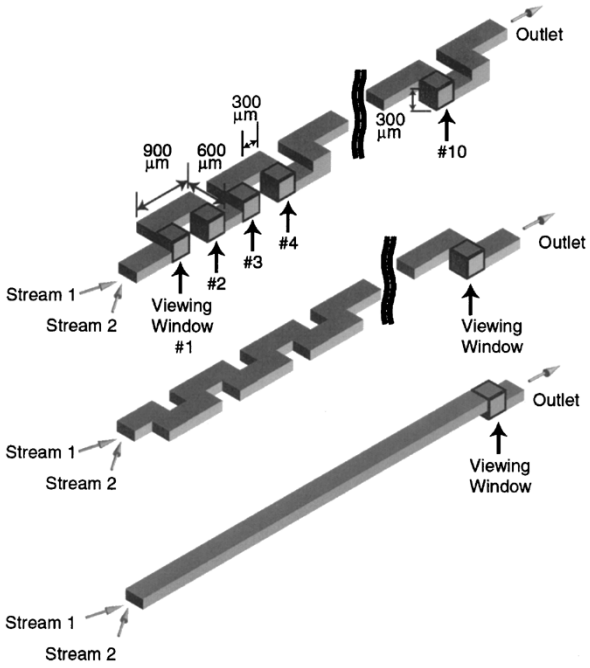

Fig. 1. (top) Schematic of the three-dimensional serpentine channel. "Viewing windows" in the channel are labeled 1–10. (middle) Schematic of square-wave channel. (bottom) Schematic of straight channel.

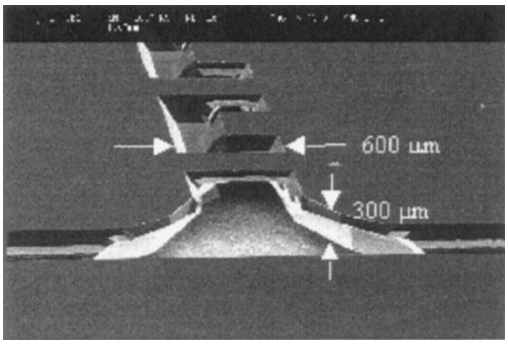

(a)

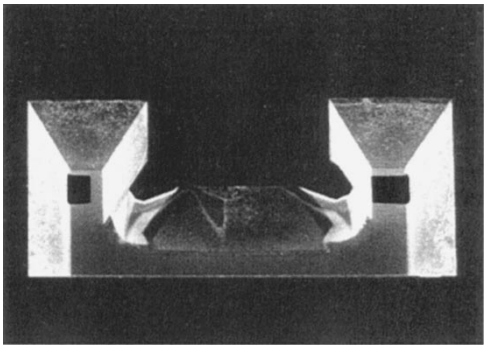

(b)

Fig. 2. (a) SEM photograph of a KOH-etched serpentine channel, including the T-junction at the inlet. (b) SEM photograph of a single channel segment. The compensation shapes at the convex corners are not completely etched away.

tion results. However, in order for the channel to be easily fabricated and integrated into existing microfluidic systems, the geometry should remain relatively simple. It is the optimization of these competing factors that drives our design.

Fig. 1(top) shows a schematic of the three-dimensional serpentine channel geometry. The basic building block of this geometry is a "C-shaped" section that turns the fluid through 180° and lies in a plane. The channel guides the fluid through an in-plane C-shaped section, rotates the fluid by 90°, and then guides the fluid through another in-plane C-shaped section. The planes of two successive C-shaped sections are perpendicular to one another. Two successive C-shaped sections will be referred to as a *mixing segment*. The serpentine micromixer tested consists of two inlet channels joined in a T-junction, a 7.5-mm-long straight channel, and a sequence of six mixing segments.

A "square-wave" channel, similar to the "zig-zag" channel tested by Branebjerg *et al.* [20], and a straight channel were also fabricated and tested to provide a comparison for evaluating the performance of the serpentine channel. Schematics of these channels are shown in Fig. 1(middle) and (bottom), respectively. Both channels have a T-junction joining two inlet channels. In the square-wave channel, the T-junction is followed by a 1-mm-long straight section and a sequence of seven mixing segments. Normally, these two channel designs would require etching from only one side of the wafer. However, in order to obtain an image of the channel cross section, as is needed for the optical measurements, it is necessary for both of these channels to be fabricated with a "viewing window." Viewing windows occur naturally in the serpentine channel, as illustrated in Fig. 1(top). A similar viewing window is fabricated in both the straight and square-wave channels, as shown in Fig. 1(middle) and (bottom), to allow equitable comparisons between all three channel geometries. Ideally these windows would be positioned so that the fluid travels the same distance through each channel from the T-junction to the viewing window. As an approximation, the windows are placed 18 mm from the T-junction as measured along the center line of each channel. Window 10 in the serpentine channel [see Fig. 1(top)] is also 18 mm from the T-junction. The straight sections in the square-wave and serpentine channels are different lengths so that these channels have the same number of 90° turns over the 18-mm length.

Common KOH anisotropic etching techniques were used to fabricate the channels in silicon wafers. The channel cross sections are all 300-μm wide at the surface of the wafer and 150-μm deep. The trapezoidal shape of the channel cross section is determined by the anisotropic nature of KOH etching. Since KOH tends to undercut the mask when etching convex corners, a square (190 μm $\times$ 190 μm) "compensation pattern" [21] was used in this design to achieve sharp convex corners. Scanning electron microscope (SEM) photographs of the resulting serpentine channel geometry are shown in Fig. 2.

A schematic illustration of the fabrication process is shown in Fig. 3. A 1-μm-thick protective coating of Si_3N_4 was first deposited on both sides of a 300-μm-thick double-side polished silicon (100) wafer using low-pressure chemical vapor deposition (LPCVD). A 500-Å film of chromium was then deposited using a sputtering system at 300 W and a pressure of 10 mtorr using argon at a flowrate of 50 sccm for 3 min. On the top side of the wafer, the chromium was patterned using a chromium etchant (CEN-300, Microchrome Technology Inc., San Jose, CA) for 1.5 min, and the Si_3N_4 was etched by reactive ion etching (RIE) at 150 W and a pressure of 50 mtorr using CF_4 at a flowrate of 50 sccm for 15 min. Next, the other side of the wafer

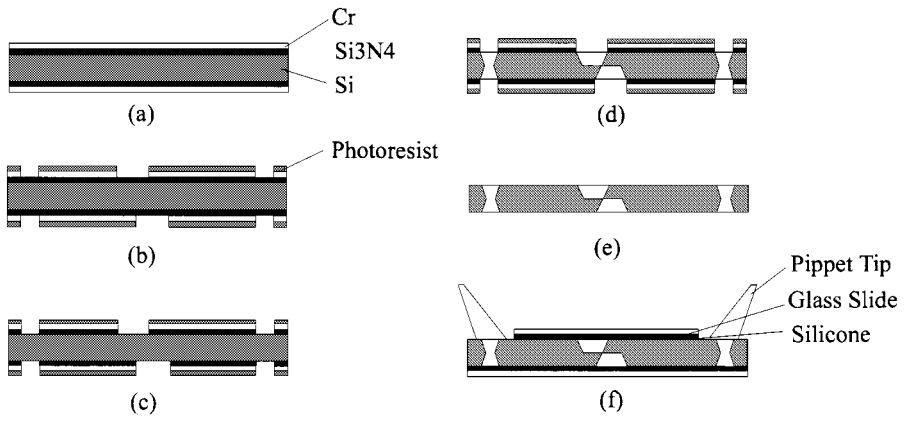

Fig. 3. Diagram of the channel fabrication process. (a) Deposit Cr. (b) Photolithography. (c) RIE etching. (d) KOH etching. (e) Stripping. (f) Packaging.

was patterned using backside alignment and a liftoff process. A 500-Å layer of chromium was sputtered and patterned on top of the AZ 5214 using the liftoff process and the Si_3N_4 on this side was etched by RIE. The wafer was then etched from both sides with a 22.5% concentration of KOH at 75 °C. After the etching process was complete, the wafer was sealed by 150-μm-thick glass cover slips (Corning Glassworks Inc., Corning, NY) using a 10-μm layer of silicone adhesive (GE Silicone, General Electric Company, Waterford, NY). The silicon adhesive was first spun on the glass cover slip (1000 r/min for 30 s). The cover slip was then soft baked at 80 °C for 10 min. After baking, the cover slip was bonded to the Si wafer followed by a hard bake at 100 °C for 10 min. The cover slips provide optical access for the intensity measurements discussed in the following section and for identifying blockages and air bubbles. Finally, pipette tips were bonded ("5 Minute" epoxy, GC Electronics, Rockford, IL) to the inlet and outlet wells.

III. Experimental Apparatus and Procedure

Mixing on the microscale is commonly evaluated by observing color or intensity variations of a dye or pH indicator as it is transported through a mixer. Indicators used include bromothymol blue [20], [22], fluorescein [23], potassium permanganate [11], rhodamine and uranine dyes [12], and phenolphthalein [10]. We have chosen to use phenolphthalein, a pH indicator that changes from colorless to red for pH values greater than eight [24]. This indicator has also been used to study mixing on the macroscale [24], [25].

Two separate fluid streams flow into each channel through the T-junction. One stream contains phenolphthalein dissolved in 99% ethyl alcohol with a concentration of approximately 0.31 mol/L. The second stream contains 98.3% sodium hydroxide pellets dissolved in 99% ethyl alcohol with a concentration of approximately 0.33 mol/L, which gives a pH of approximately 13. This high concentration of NaOH was used to obtain a large color change in the phenolphthalein. Despite the high pH value, no reactions were observed between the sodium hydroxide stream and the silicon wafer.

The phenolphthalein and sodium hydroxide streams are introduced into the mixer from syringes connected by tubes to the inlet pipettes. The volumetric flowrates in these streams are controlled simultaneously by a Harvard Apparatus PHD 2000 syringe pump. Flowrates produced by this syringe pump are slightly unsteady. Root-mean-square pressure fluctuations of 3.2% were observed in a straight channel at an Re of approximately five, with the degree of unsteadiness appearing to decrease with increasing flow rate. After the two colorless streams come in contact, both sodium hydroxide and phenolphthalein begin to diffuse. The reaction time of the phenolphthalein is negligible [26], although the ratio of reacted-to-unreacted phenolphthalein at any point within the device depends on the local pH value in a nontrivial way [25]. Thus, the amount of reacted phenolphthalein produced (and, hence, the intensities reported in the following section) depends on the diffusivities and initial concentrations of both phenolphthalein and sodium hydroxide.

The mixing ability of the device is quantified by optically determining how much of the phenolphthalein changes color during the mixing process. Images of the reacted phenolphthalein are captured through an Olympus BX60 microscope at 40 times magnification with a Sony 8-bit charge-coupled device (CCD) camera. The microscope lens has a depth-of-focus of 7 μm at this magnification. Illumination comes from a halogen light source mounted behind the mixer. This setup gives clear images of the red phenolphthalein, but only allows images to be obtained at positions where the silicon wafer is etched completely through. Since the halogen lamp produces incoherent light, the light waves scattered by two molecules have additive intensities when the images of the molecules overlap. Thus, the intensity of red integrated over a window image is proportional to the amount of reacted phenolphthalein in the imaged volume. This intensity is given by $I = \sum_{i=1}^{N} I_i$, where I_i is the intensity of red in pixel i and N is the total number of pixels in the window image. Since the cross-sectional area of each viewing window may be slightly different, the pixel-averaged intensity $\bar{I} = I/N$ is used to compare between viewing windows. Additionally, the actual intensity values are dependent on the CCD camera and light source used, thus all intensities are normalized by $I_{\max}$, which is determined empirically as the maximum intensity observed in any pixel in a fully mixed image such as Fig. 4(f). Our experimental setup allows us to measure changes in intensity at each pixel of approximately 0.5% of full scale.

Mixing in these channels can also be evaluated by considering the uniformity of the intensity in the imaged fluid volume. The uniformity can be quantified by calculating the deviation of the pixel intensity values I_i in a given image from the maximum intensity value

$$D_I = \sqrt{\frac{1}{N}\sum_{i=1}^{N}(I_i - I_{\max})^2}. \quad (1)$$

A fully mixed channel will have $D_I = 0$. If a conserved quantity were being mixed, the appropriate measure would be the standard deviation, i.e., the deviation about the mean intensity $\bar{I}$. However, since the amount of red phenolphthalein increases as the fluid moves downstream, the standard deviation does not give an accurate representation of mixing uniformity. Also, if the red phenolphthalein is in a thin sheet viewed edge-on, the intensity is zero in almost every pixel in the image, and both $\bar{I}$ and the standard deviation are approximately zero. However, the streams are obviously not well mixed. For these reasons, we use the deviation defined in (1). As with the intensity, the actual deviation values depend on the CCD camera and light source used, so the deviation is normalized by $I_{\max}$. It is also important to note that both the intensity and deviation are dependent on the channel depth that is imaged. However, all of our channels are 300-μm deep at a viewing window, so this dependence does not affect our comparisons.

The way in which the mixing device distorts an interface in the flow is also visualized by using a stream of pure deionized water and a stream of 99% ethyl alcohol. The density difference between these two fluids causes light to refract at their interface. The resulting images are captured with the CCD camera.

IV. Results

The design of the three-dimensional serpentine channel allows images of the phenolphthalein reaction to be obtained at two locations in each mixing segment, providing a picture of how mixing progresses as the fluids move downstream. Example intensity images from three different channel positions are shown in Fig. 4 for two different values of Reynolds number. Two observations can be made immediately from these images: 1) the interface between streams is distorted as it moves downstream and 2) the mixing rate in the channel increases with increasing Reynolds number. The mixing ability of this channel is illustrated by the following comparison. Mixing by pure diffusion has been measured in this channel to take approximately 3 s, but the two streams have been in contact an average of only 0.03 s by the time they reach the window shown in Fig. 4(f).

The interface between the streams is difficult to determine from Fig. 4 because diffusion quickly smooths out the images. A clearer visualization of the interface is possible by using streams of deionized water and ethyl alcohol, as shown in Fig. 5. A significant amount of "stirring" is being accomplished by the geometry of the serpentine channel. This stirring is a continuous deformation of a smooth interface, so while very thin striations may result, the interface will not be made to intersect itself. The apparent self-intersections of the interfaces that appear in Fig. 5

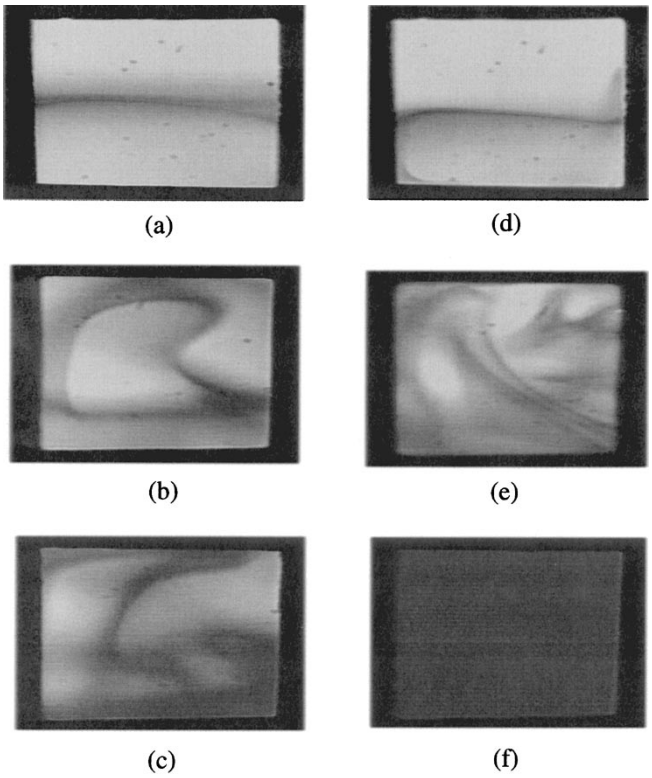

Fig. 4. Photographs of reacted phenolphthalein in the serpentine channel with $\mathrm{Re} = 12$ ($Q = 0.2$ mL/min) at window: (a) one, (b) two, and (c) four; and with $\mathrm{Re} = 70$ ($Q = 1.2$ mL/min) at window: (d) one, (e) two, and (f) four. Window locations are shown in Fig. 1(top).

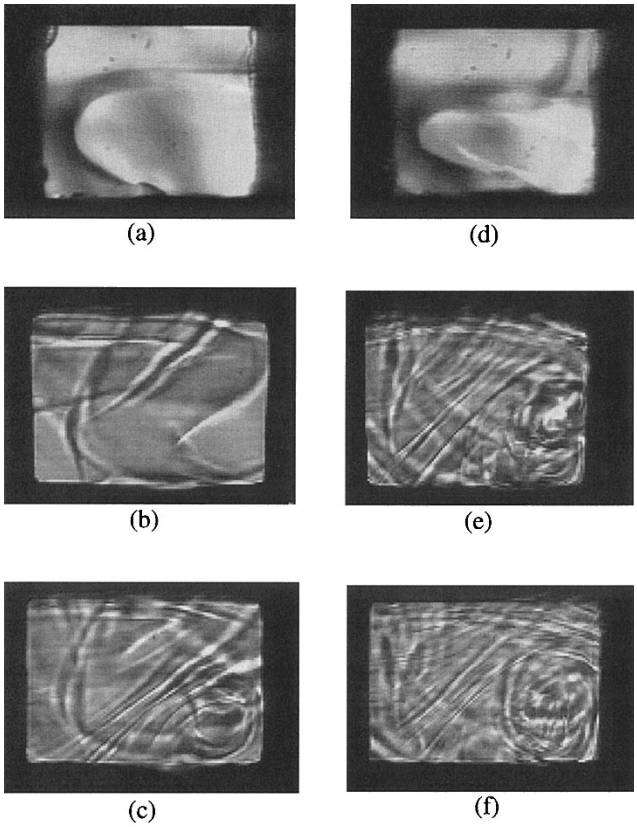

Fig. 5. Photographs of the water–alcohol interface in the serpentine channel with $\mathrm{Re} = 23$ ($Q = 0.4$ mL/min) at window: (a) one, (b) two, and (c) four; and with $\mathrm{Re} = 70$ ($Q = 1.2$ mL/min) at window: (d) one, (e) two, and (f) four. Window locations are shown in Fig. 1(top).

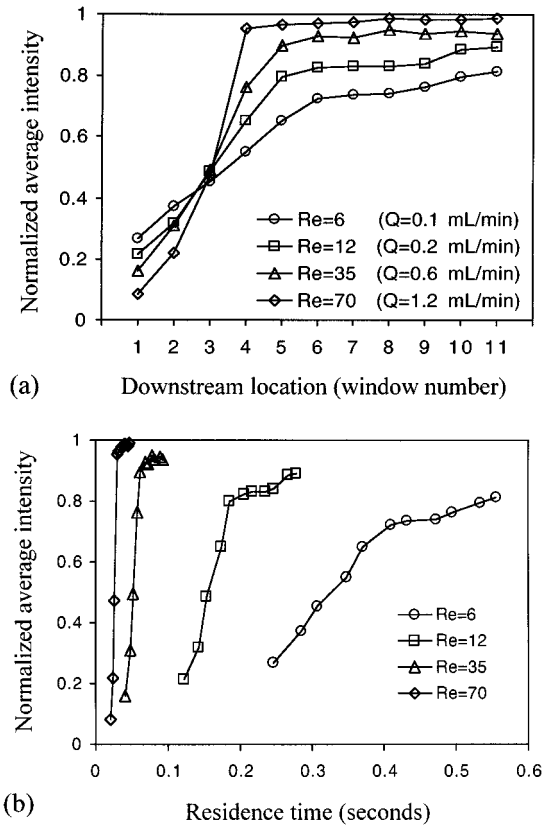

Fig. 6. (a) Normalized average intensity $\bar{I}/I_{\max}$ in each window of the serpentine channel for various Reynolds numbers. Window locations are shown in Fig. 1(top). (b) Normalized average intensity in each window of the serpentine channel as a function of residence time.

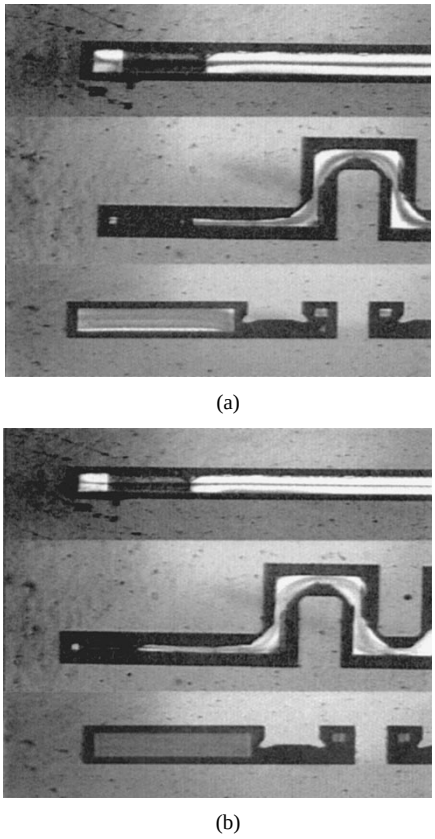

Fig. 7. Photographs of side-by-side flow experiments comparing the straight channel, square-wave channel, and serpentine channel. (a) Flowrate is 0.2 mL/min ($\mathrm{Re} = 12$). (b) Flowrate is 1.2 mL/min ($\mathrm{Re} = 70$).

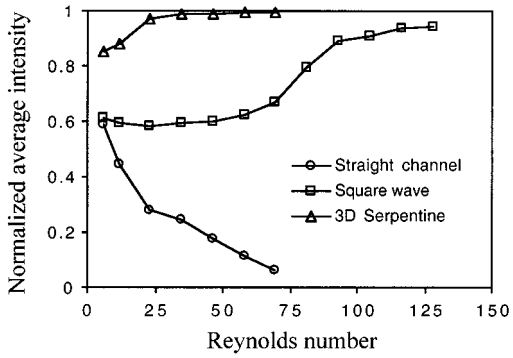

Fig. 8. Normalized average intensity $\bar{I}/I_{\max}$ in each channel 18 mm beyond the T-junction for various Reynolds numbers.

are primarily due to each image being a two-dimensional projection of a three-dimensional interface. Note that, because water and alcohol have different densities, one does not expect the interfaces in Figs. 4 and 5 to be identical.

Normalized average intensity values from each window in the serpentine channel are shown in Fig. 6(a) for four different Reynolds numbers. The intensity at window #1 indicates the amount of mixing that has taken place before the streams enter the first mixing segment. Mixing in the initial 7.5-mm-long straight section is dominated by diffusion, so the longer the streams stay in this section (i.e., the lower the Re) the more mixed they become. This dependence on residence time[2] is illustrated in Fig. 6(b). After the streams enter the mixer, however, the mixing rate, which is given by the slope of the intensity curve, increases with increasing Reynolds number. In all cases, the mixing rate levels off after two or three mixing sections. At $\mathrm{Re} = 70$, mixing in the serpentine channel produces essentially the maximum amount of reacted phenolphthalein after only two mixing segments.

Fig. 7 shows results of experiments with phenolphthalein and sodium hydroxide solutions performed simultaneously in the straight channel, square-wave channel, and three-dimensional serpentine channel. These images illustrate the mixing capability of the serpentine channel. This capability is quantified in Fig. 8 by comparing the average intensity of reacted phenolphthalein present in each of the three channels after the streams have been in contact for 18 mm (measured along the center line of each channel). Mixing in the straight channel decreases rapidly with increasing Reynolds number due to the corresponding decrease in residence time. The behavior of the straight channel shows the inverse relationship between diffusion-dominated mixing and Reynolds number. Mixing in the square-wave channel is almost solely by molecular diffusion at $\mathrm{Re} = 6$ and varies only slightly with the Reynolds number until $\mathrm{Re} = 70$, after which mixing increases significantly. A maximum intensity of 94% is observed in this channel at Reynolds number of 140. In the serpentine channel, mixing increases rapidly with Reynolds number, with 97% of the maximum intensity observed at $\mathrm{Re} = 25$. At $\mathrm{Re} = 70$, the

[2]Residence time is defined here as the center-line length of the channel divided by the average flow velocity.

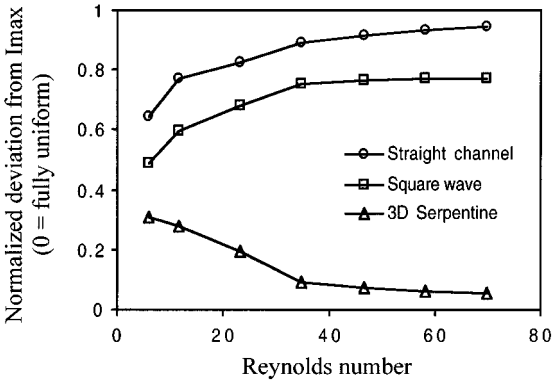

Fig. 9. Uniformity of mixing in each channel at various Reynolds numbers as measured by a normalized deviation of the intensity from $I_{\max}$.

square-wave channel produces ten times as much red dye as the straight channel, while the serpentine channel produces 16 times more product than the straight channel and 1.6 times more product than the square-wave channel.

Mixing in these channels is also quantified by examining the uniformity of reacted phenolphthalein in the imaged volumes. Fig. 9 shows the normalized deviation of intensity $D_I/I_{\max}$ in the three channel geometries for Reynolds numbers from 6 to 70. The straight channel shows a continual increase in deviation with increasing Re. The square-wave channel follows a similar trend, although it does mix better than the straight channel and the deviation begins to level out after $\mathrm{Re} = 35$. Deviation in the serpentine channel decreases continually with increasing Re, and the values are significantly lower than those from the other two channels.

V. Discussion

Fluid flows in microfluidic devices are predominantly laminar, with Reynolds numbers typically ranging from 0.01 to 100 [1]–[3]. At the lowest Reynolds numbers, $0.01 < \mathrm{Re} < 1$, viscous forces in the fluid dominate inertial forces, and fluid velocities in a channel cross section are essentially two-dimensional. Mixing enhancement in this regime can be achieved by adding complexity to the system, such as "laminating" the fluid [10] or introducing time-dependent forcing. Fortunately, at this scale, the typical dimension of a microchannel cross section is tens of micrometers (especially in microelectophoretic systems), and pure molecular diffusion can complete mixing in a few seconds. Here we investigate mixing improvements in microsystems for $1 < \mathrm{Re} < 100$. In this range of Reynolds numbers, both viscous and inertial forces are important. As a result, flow around a channel bend will be three-dimensional, with "secondary flows" being generated in the channel cross section in addition to the bulk flow along the axis of the channel. These secondary flows, in combination with the axial flow, distort and stretch material interfaces and can produce chaotic advection. As a result, the interfacial area across which diffusion occurs is greatly increased, which leads to rapid mixing.

Since viscous flow around a bend generates a three-dimensional velocity field, secondary flows do occur in the square-wave channel. However, the results in Fig. 8 show that at $\mathrm{Re} = 6$ the effect of these secondary flows is negligible, and mixing is essentially by diffusion only. As the Reynolds number is increased, the flow in this channel becomes increasingly three-dimensional, but initially this increase is only enough to maintain a relatively constant amount of mixing. This behavior suggests that little or no chaotic advection is produced in the square-wave channel for $\mathrm{Re} < 70$. The improved mixing shown in Fig. 8 for $\mathrm{Re} > 70$ indicates that there is a significant increase in the complexity of the flow for these Reynolds numbers. This complexity may be due to a large increase in the strength of the secondary flows or to the onset of unsteady flow in the channel. Unsteadiness can be introduced through flow separation at the inside corners of each square-wave section. As the Reynolds number is increased, separated flows typically become unstable, leading to oscillations in the flow field. Numerical modeling and further experimentation are currently being done to better understand the flow in the square-wave channel at the higher Reynolds numbers.

The distortion of the interfaces shown in Fig. 4 demonstrates that, even at the lower Reynolds numbers, the twisting and turning of the flow through the serpentine channel generates strong secondary flows that produce significant stretching in the fluid. This distortion and the mixing results shown in Fig. 6 are consistent with the occurrence of chaotic advection in the serpentine channel throughout the entire range of Reynolds number tested.

The mixing enhancement achieved in the serpentine channel is, to some degree, independent of the quantities being mixed, as stirring of the flow by chaotic advection depends on the velocity field and not on the diffusivity of the species involved. In contrast, mixing in the square-wave channel at the lower Reynolds numbers is dominated by diffusion. Since the diffusion of phenolphthalein and sodium hydroxide is quite fast compared to many of the molecules that are mixed in microsystems, we anticipate that the difference demonstrated here between the serpentine channel and the square-wave channel would be more dramatic if molecules with lower diffusivities were used.

The SEM photographs in Fig. 2 show that the shape of the channel cross section results in "necking" of the serpentine channel as it passes from one side of the wafer to the other. When compared with a similar channel having orthogonal walls, these narrow openings will increase the pressure drop needed to maintain a given flowrate, cause larger local deformations in the fluid, and increase the chances of clogging the channel. However, preliminary numerical models indicate that this necking is not a necessary part of the design [27]. These narrow openings can be eliminated by using a different fabrication technique such as deep reactive ion etching (DRIE) of silicon or micromolding techniques [28].

VI. Conclusion

Flow visualization experiments confirm that the three-dimensional serpentine channel mixes significantly better than the square-wave channel and a straight channel for Reynolds numbers from 6 to 70. Mixing in the serpentine channel relies on the flow field being sufficiently three-dimensional, with secondary flows stretching and folding the fluid, greatly

increasing the interfacial area across which diffusion occurs. The experimental results suggest the occurrence of chaotic advection in the serpentine micromixer. At a Reynolds number of 70, the serpentine channel produces 16 times more reacted phenolphthalein than a straight channel and 1.6 times more than the square-wave channel. More detailed experiments and numerical simulations are currently being performed that will provide us with a better understanding of the mixing process in these channels and improve our ability to "design for chaos."

The passive three-dimensional serpentine micromixer has a number of advantages that makes it attractive for use in a wide variety of microfluidic applications. First, this channel is easy to fabricate and integrate with other microfluidic components, as the design is relatively simple and can be manufactured using any one of several different microfabrication techniques. The results shown here are for essentially steady flow, but using this mixer in an application with time-dependent flow should enhance, not degrade, its performance. There is also some flexibility in the choice of channel geometry, as the occurrence of chaotic advection is not specific to the serpentine channel presented here. We are currently examining other channel designs. Secondly, the occurrence of chaotic advection depends on the global three-dimensionality of the flow field, not on high local rates-of-strain. Thus, using chaotic advection to mix biomolecular streams may help minimize damage to large biomolecules, some of which are particularly prone to shear-induced damage [29]. Finally, keeping the flow in a single channel with a height-to-width ratio near one maintains a relatively low surface-to-volume ratio, which minimizes the chances of clogging, fouling, and loss of sample by biomolecular adsorption onto the device surface.

REFERENCES

[1] R. C. Anderson, G. J. Bogdan, A. Puski, and X. Su, "Genetic analysis systems: Improvements and methods," in *Proc. Solid-State Sens. Actuator Workshop*, Hilton Head, SC, 1998, pp. 7–10.

[2] C. Bisson, J. Campbell, R. Cheadle, M. Chomiak, J. Lee, C. Miller, C. Milley, P. Pialis, S. Shaw, W. Weiss, and C. Widrig, "A microanalytical device for the assessment of coagulation parameters in whole blood," in *Proc. Solid-State Sens. Actuator Workshop*, Hilton Head, SC, 1998, pp. 1–6.

[3] N. Chiem, C. Colyer, and J. D. Harrison, "Microfluidic systems for clinical diagnostics," in *Proc. Int. Solid-State Sens. Actuators Conf.*, Chicago, IL, 1997, pp. 183–186.

[4] K. F. Jensen, S. L. Firebaugh, A. J. Franz, D. Quiream, R. Srinivasan, and M. A. Schmidt, "Integrated gas phase microreactors," in *Proc. 3rd Int. Miniaturized Anal. Syst. Symp.*, Banff, Alta., Canada, 1998, pp. 463–468.

[5] R. F. Service, "Miniaturization puts chemical plants where you want them," *Science*, vol. 282, p. 400, 1998.

[6] J. B. Brody and P. Yager, "Low Reynolds number micro-fluidic devices," in *Proc. Solid-State Sens. Actuator Workshop*, Hilton Head, SC, 1996, pp. 105–108.

[7] J. Evans, D. Liepmann, and A. P. Pisano, "Planar laminar mixer," in *Proc. IEEE MEMS Workshop*, Nagoya, Japan, 1997, pp. 96–101.

[8] H. T. Evensen, D. R. Meldrum, and D. L. Cunningham, "Automated fluid mixing in glass capillaries," *Rev. Sci. Inst.*, vol. 69, pp. 519–526, 1998.

[9] R. M. Moroney, R. M. White, and R. T. Howe, "Ultrasonically induced microtransport," in *Proc. IEEE MEMS Workshop*, Amsterdam, The Netherlands, 1991, pp. 277–282.

[10] J. Branebjerg, P. Gravesen, J. P. Krog, and C. R. Nielsen, "Fast mixing by lamination," in *Proc. IEEE MEMS Workshop*, San Diego, CA, 1996, pp. 441–446.

[11] H. Mensinger, T. Richter, V. Hessel, J. Döpper, and W. Ehrfeld, "Microreactor with integrated static mixer and analysis system," in *Proc. Micro Total Anal. Syst. Workshop*, Enschede, The Netherlands, 1994, pp. 237–243.

[12] R. Miyake, T. S. J. Lammerink, M. Elwenspoek, and J. H. J. Fluitman, "Micro mixer with fast diffusion," in *Proc. IEEE MEMS Workshop*, Ft. Lauderdale, FL, 1993, pp. 248–253.

[13] S. W. Jones, O. M. Thomas, and H. Aref, "Chaotic advection by laminar flow in a twisted pipe," *J. Fluid Mech.*, vol. 209, pp. 335–357, 1989.

[14] H. Aref, "Stirring by chaotic advection," *J. Fluid Mech.*, vol. 143, pp. 1–21, 1984.

[15] ——, "Chaotic advection of fluid particles," *Philos. Trans. R. Soc. London A, Math. Phys. Sci.*, vol. 333, pp. 273–288, 1990.

[16] N. Acharya, M. Sen, and H.-C. Chang, "Heat transfer enhancement in coiled tubes by chaotic mixing," *Int. J. Heat Mass Transf.*, vol. 35, pp. 2475–2489, 1992.

[17] A. Mokrani, C. Castelain, and H. Peerhossaini, "The effect of chaotic advection on heat transfer," *Int. J. Heat Mass Transf.*, vol. 40, pp. 3089–3104, 1997.

[18] D. Sawyers, M. Sen, and H. Chang, "Effect of chaotic interfacial stretching on bimolecular chemical reaction in helical-coil reactors," *Chem. Eng. J*, vol. 64, pp. 129–139, 1996.

[19] R. H. Liu, K. V. Sharp, M. G. Olsen, M. A. Stremler, J. G. Santiago, R. J. Adrian, H. Aref, and D. J. Beebe, "A passive micromixer: Three-dimensional serpentine microchannel," in *Tech. Dig. Int. Solid-State Sens. Actuators Conf*, Sendai, Japan, 1999, pp. 730–733.

[20] J. Branebjerg, B. Fabius, and P. Gravesen, "Application of miniature analyzers: From microfluidic components to μTAS," in *Proc. Micro Total Anal. Syst. Workshop*, Enschede, The Netherlands, 1994, pp. 141–151.

[21] B. Puers and W. Sansen, "Compensation structures for convex corner micromachining in silicon," *Sens. Actuators*, vol. A21–A23, pp. 1036–1041, 1990.

[22] A. Desai, D. Bökenkamp, X. Yang, Y.-C. Tai, E. Marzluff, and S. Mayo, "Microfluidic sub-millisecond mixers for the study of chemical reaction kinetics," in *Proc. Int Solid-State Sens. Actuators. Conf.*, Chicago, IL, 1997, pp. 167–170.

[23] J. Voldman, M. L. Gray, and M. A. Schmidt, "Liquid mixing studies with an integrated mixer/valve," in *Proc. 3rd Int. Miniaturized Anal. Syst. Symp.*, Banff, Alta., Canada, 1998, pp. 181–184.

[24] R. Breidenthal, "Structure in turbulent mixing layers and wakes using a chemical reaction," *J. Fluid Mech.*, vol. 109, pp. 1–24, 1981.

[25] S. Zhang, S. P. Schneider, and S. H. Collicott, "Quantitative molecular-mixing measurements using digital processing of absorption images," *Exp. Fluids*, vol. 19, pp. 319–327, 1995.

[26] E. F. Caldin, *Fast Reactions in Solution*. New York: Wiley, 1964, pp. 66–67.

[27] M. A. Stremler and H. Aref, "Chaotic advection in a static microscale mixer," *Bull. Amer. Phys. Soc.*, vol. 43, p. 2131, 1998.

[28] B. H. Jo, L. VanLerberghe, K. Motsegood, and D. J. Beebe, "Fabrication of three-dimensional microfluidic systems by stacking molded PDMS layers," in *Proc. SPIE Micromach. Microfabrication Symp.*, Santa Clara, CA, 1999, pp. 222–229.

[29] D. Leckband and G. Hammes, "Interactions between nucleotide binding sites on chloroplast coupling factor one during ATP hydrolysis," *Biochem.*, vol. 26, pp. 2306–2312, 1997.

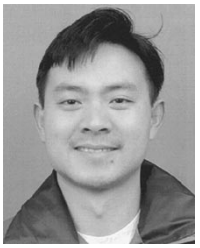

Robin H. Liu received the B.S. degree in mechanical engineering from the South China University of Technology, Guang Zhou, China, in 1991, the M.Sc. degree from the Louisiana Technical University, Ruston, in 1996, and is currently working toward the Ph.D. degree in mechanical engineering at the University of Illinois at Urbana-Champaign.

He was a Summer Intern at Aclara Biosciences Inc., in 1999. He is currently a Research Assistant at the Beckman Institute for Advanced Science and Technology, University of Illinois at Urbana-Champaign. His research interests include LIGA (synchrotron radiation lithography, electroforming, and micromolding) technology with applications to microoptical components, development of tactile sensors, microfluidic components (e.g., mixers, valves, sensors, etc.) and systems (e.g., pH self-regulation system), functional materials, and biochemistry.

Mark A. Stremler received the B.S. degree in mechanical engineering and the B.S. degree in mathematics from the Rose-Hulman Institute of Technology, Terre Haute, IN, in 1993, and the M.S. and Ph.D. degrees in theoretical and applied mechanics from the University of Illinois at Urbana-Champaign, in 1995 and 1998, respectively.

He is currently a Post-Doctoral Research Associate at the Beckman Institute for Advanced Science and Technology, University of Illinois at Urbana-Champaign. His research interests are in theoretical and computational fluid mechanics and applied mathematics, including microfluidics and chaotic advection.

Kendra V. Sharp received the B.S. degree in aeronautical and astronautical engineering from the University of Illinois at Urbana-Champaign, in 1993, the M.Phil. degree in engineering from Cambridge University, Cambridge, U.K., in 1994, the M.Eng. degree in mechanical engineering from the University of California at Berkeley, in 1996, and is currently working toward the Ph.D. degree in theoretical and applied mechanics at the University of Illinois at Urbana-Champaign.

Her research focuses on experimental fluid mechanics, particularly two-phase flows and mixing at the microscale.

Michael G. Olsen received the B.S., M.S., and Ph.D. degrees in mechanical engineering from the University of Illinois at Urbana-Champaign, in 1992, 1995, and 1999, respectively. His Ph.D. research involved planar velocity measurements in both incompressible and weakly compressible mixing layers.

He is currently a Post-Doctoral Research Associate at the Beckman Institute for Advanced Science and Technology, University of Illinois at Urbana-Champaign. His current research interests include developing experimental techniques such as particle image velocimetry for microfluidics, design and testing of microfluidic components, and the flow of non-Newtonian fluids in microfluidic devices.

Juan G. Santiago received the B.S. degree in mechanical engineering from the University of Florida, Gainesville, in 1990, and the M.S. and Ph.D. degrees in mechanical engineering from the University of Illinois at Urbana-Champaign, in 1992 and 1995, respectively.

He was a Senior Member of the Technical Staff at the Aerospace Corporation from 1995 to 1997 and a Research Scientist at the Beckman Institute for Advance Science and Technology, University of Illinois at Urbana-Champaign from 1997 to 1998. He is currently an Assistant Professor of Mechanical Engineering at Stanford University, Stanford, CA. His research interests include microscale fluid mechanics, microscale optical flow diagnostics, and microfluidic system design and fabrication.

Ronald J. Adrian received the B.M.E. and M.S. degrees in mechanical engineering from the University of Minnesota at Minneapolis-St. Paul, in 1967 and 1969, respectively, and the Ph.D. degree in physics from Cambridge University, Cambridge, U.K., in 1972.

He was an Assistant Professor (1972–1977) and an Associate Professor (1977–1981) at the University of Illinois at Urbana-Champaign. He is currently the Hoeft Professor of Engineering at the University of Illinois at Urbana-Champaign, and Director of the Laboratory for Turbulence and Complex Flow, Department of Theoretical and Applied Mechanics. His research interests are the space–time structure of turbulent fluid motion and the development of techniques, both experimental and mathematical, to explore this structure. Methods to which he has made fundamental contributions are the laser Dopplet velocimeter technique, the method of particle image velocimetery, and the stochastic estimation method.

Hassan Aref received the Cand. Scient. degree in physics from the University of Copenhagen, Copenhagen, Denmark, in 1975, and the Ph.D. degree in physics from Cornell University, Ithaca, NY, in 1980.

He was an Assistant Professor (1980–1984) and an Associate Professor (1984–1985) at Brown University, Providence, RI. He was an Associate Professor (1985–1988) and a Professor (1988–1992) at the University of California at San Diego. He is currently a Professor of Theoretical and Applied Mechanics and the Interim Chief Information Officer at the University of Illinois at Urbana-Champaign. His research interests include theoretical and computational fluid mechanics, vortex dynamics, applications of chaos, and foams.

David J. Beebe (S'89–M'90) received the B.S., M.S., and Ph.D. degrees in electrical engineering from the University of Wisconsin-Madison, in 1987, 1990, and 1994, respectively.

He was an Electrical Engineer for the Kimberly-Clark Corporation (1987–1989), an NIH Biotechnology Predoctoral Trainee (1991–1994), and an Assistant Professor at the Louisiana Technical University (1994–1996). He was an Assistant Professor in the Department of Electrical and Computer Engineering, University of Illinois at Urbana-Champaign, and an Assistant Research Professor at the Beckman Institute for Advanced Science and Technology. In January 2000, he joined the faculty in the Department of Biomedical Engineering, University of Wisconsin-Madison. His research interests are in biomedical instrumentation and the development of microfabricated devices for biomedical applications, including technology development for the handling and analysis of biological objects, develop of novel microfluidic devices and systems, use of dendritic and functional materials in microelectromechanical systems (MEMS), development of electrostatic and electrocutaneous haptic displays, and tactile sensors.